DOI: 10.1002/adsc.202((will be filled in by the editorial staff))

Stereoselective Cyclopropanation of BODIPY Derivatives by an Organocascade Reaction

Vojtěch Dočekal,[a] Tereza Koberová,[a] Jan Hrabovský,[b,c] Róbert Gyepes,[d] Ivana Císařová,[e] Ramon Rios[f] and Jan Veselý[a*]

[a] Department of Organic Chemistry, Faculty of Science, Charles University, Hlavova 2030/8, 128 43 Prague 2, Czech Republic, E-mail: jan.vesely@natur.cuni.cz http://orgchem.cz/vesely/
[b] Faculty of Mathematics and Physics, Charles University in Prague, Prague, Czech Republic
[c] HiLASE Centre, Institute of Physics of the Czech Academy of Sciences, Dolní Břežany, Czech Republic
[d] J. Heyrovský Institute of Physical Chemistry of the Czech Academy of Sciences, Dolejškova 3, 182 23 Prague 8, Czech Republic
[e] Department of Inorganic Chemistry, Faculty of Science, Charles University, Hlavova 2030/8, 128 43 Prague 2, Czech Republic
[f] School of Chemistry, University of Southampton, Highfield Campus, SO17 1BJ Southampton, UK

Received: ((will be filled in by the editorial staff))

Supporting information for this article is available on the WWW under http://dx.doi.org/10.1002/adsc.201######.((Please delete if not appropriate))

Abstract. The synthesis of enantiopure chiral BODIPYs is of paramount importance due the intrinsic properties of BODIPYs as fluorophores that could be used as probes for molecular sensing. The present study reports an asymmetric organocatalytic cascade reaction of *meso*-chloromethyl BODIPY derivatives with *α,β*-unsaturated aldehydes catalyzed efficiently by a chiral secondary amine. The corresponding BODIPY-derived cyclopropanes were produced in isolated yields about 90% and with high stereochemical outcomes (dr >20/1, and 99% *ee*). The synthetic utility of the protocol was exemplified on a set of additional transformations of the corresponding optically pure compounds. In addition, a study explaining the reaction mechanism (DFT computations) and photophysical characterization of all enantioenriched products were accomplished.

Keywords: Asymmetric catalysis; Organocatalysis; Dyes/Pigments; Cyclization; Domino reactions

Boron-dipyrromethene (BODIPY) compounds attained enormous focus on research interest due to their excellent thermal and photochemical stability, high quantum yield, negligible triplet-state formation, intense absorption profile, good solubility, and chemical robustness.[1] During recent decades, BODIPYs have been studied extensively for their utilization in wide range of applications, such as chemosensors,[2] biological labels,[3] dye lasers, photodynamic therapy, optoelectronic devices, and chiral sensing[4]. Chirality plays an important role in this regard and could inspire the development of other applications (Figure 1, A).[5] Until now, chiral lanthanides have been almost exclusively used as circularly polarised luminescence (CPL) emitters;[6] however, these compounds have usually low fluorescence quantum yields that will lead to low overall CPL quantum efficiencies. On the other hand, BODIPYs exhibit high extinction coefficients, fluorescence quantum yields and tuneable emission properties. The possibility of synthesising enantiopure chiral BODIPYs with potentially reasonable luminescence dissymmetry factors could allow for the development of improved version of chiral lanthanides.[7] The importance of developing new and improved CPL resides in their potential applications as smart photonic applications, such as 3D displays and information storage.[8] However, despite the growing interest in chiral BODIPYs, to the best of our knowledge only few examples of methodologies leading to chiral BODIPYs have been yet developed.[9]

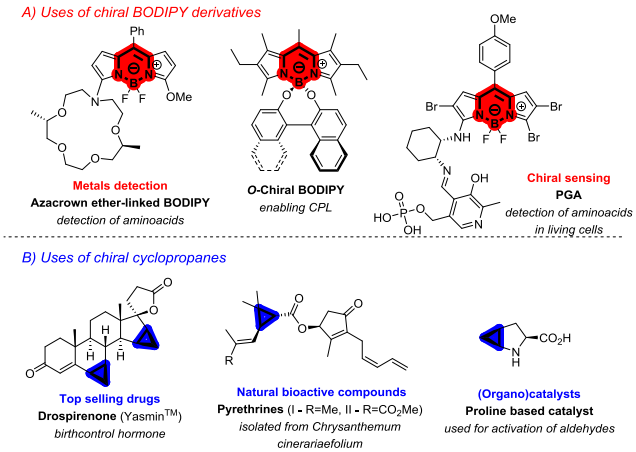

Figure 1. Selected uses of cyclopropanes and chiral BODIPY derivatives.

In 2019, Aleman and co-workers reported the first enantioselective methodology for the synthesis of chiral BODIPYs, taking advantage of their EWG properties for the activation of a conjugated double bond.[12c] In 2021, we developed an addition of BODIPYs to MBH carbonates, which showed nucleophilic character of carbon bonded to a meso position of BODIPY (Scheme 1).[12a]

Chiral cyclopropanes, the smallest cycloalkanes that possess unique structural properties are key pharmacophores in pharmaceuticals[13] and in bioactive natural products.[14] Non-surprisingly, this structural motif is present also in chiral ligands[15] and catalysts[16] (Figure 1, B). Considering the high potency of chiral cyclopropanes, significant effort has been devoted to the development of enantioselective cyclopropanation methodologies. Among catalytic methods, an organocatalytic approach was identified as highly valuable for constructing various cyclopropanes.[17] Probably the most popular organocatalytic cyclopropanation strategy involves cascade processes initiated by Michael addition of various nucleophiles bearing leaving groups (Scheme 1, B).[18] Despite the impressive advances made in organocatalytic enantioselective cyclopropanations, there is no report on the synthesis of enantiopure chiral BODIPYs anchored to rigid carbocyclic systems with well-defined spatial arrangement, allowing late-stage functionalization.

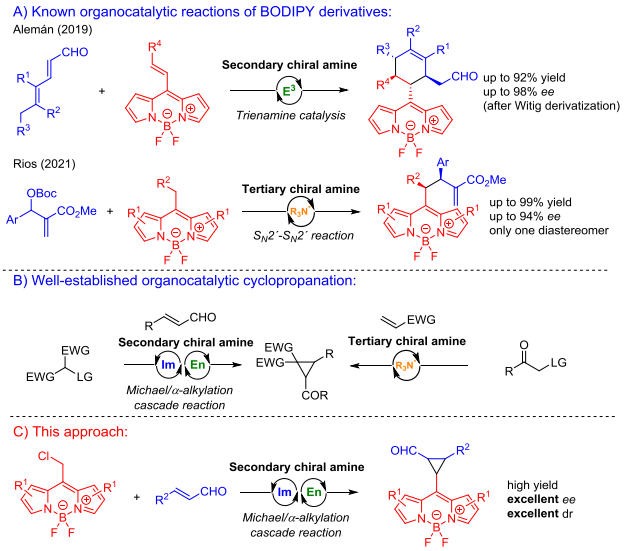

Scheme 1. Known organocatalytic reactions of BODIPY derivatives and previous approaches toward the preparation of chiral cyclopropanes.

Based on our previous results[19] we envisioned that chloro-methyl BODIPYs can react with enals under secondary amine catalysis to furnish a new class of chiral BODIPYs, which present several advantages as their easy prefunctionalization (using different pyrroles or enals) or their postfunctionalization by the addition of synthetic handles like the final aldehyde moiety.

To verify the designed strategy, we started our investigation by examining the organocatalytic cascade reaction of readily accessible chloromethyl BODIPY derivate (**1a**) with trans-cinnamaldehyde (**2a**) in the presence of proline-based Hayashi/Jørgensen catalyst **C1** and $NaHCO_3$ as a base. Fortunately, the reaction proceeded smoothly to deliver desired cyclopropane (**3a**) in a high isolated yield with high diastereocontrol and excellent enantiopurity (entry 1, Table 1). Diastereoselectivity was slightly increased when pyridine (entry 2) and pyridine-like bases, such as 2,6-lutidine (entry 3), were used. Satisfyingly, the reaction showed increased stereocontrol with diphenylprolinol-derived catalysts **C2** and **C3** bearing bulkier silyl group (entry 4, 5). Conversely, the diastereocontrol of the reaction catalyzed by **C4** was significantly diminished. The model reaction catalyzed by commercially available Jørgensen catalyst **C5** (entry 7) produced cyclopropane **3a** in nearly quantitative yield as a single optically pure diastereomer. Apart from **C1**-**C7**, we tested other secondary amine catalysts (for details, please see the SI file) solvents and other reaction conditions, but no further improvement of reaction efficiency was observed. On the other hand, we found the same efficiency and stereocontrol of model reaction with a lowered amount of aldehyde and catalyst (entry 13). For complete optimization studies, please, see the SI file.

Table 1. Optimization of the reaction conditions.

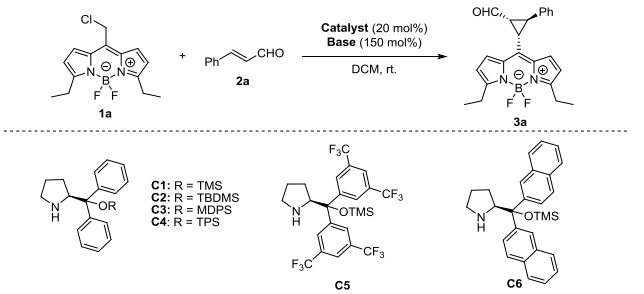

Entry[a]	Cat.	Base	Time (h)	Dr[b]	Yield[c] (%)	*ee*[d] (%)
1[e]	**C1**	$NaHCO_3$	15	8/1	70	99
2	**C1**	pyridine	90	10/1	88	99
3	**C1**	lutidine	15	12/1	92	98
4	**C2**	lutidine	15	12/1	75	99
5	**C3**	lutidine	15	19/1	90	99
6	**C4**	lutidine	15	5/1	72	99
7	**C5**	lutidine	15	>20/1	95	99
8	**C6**	lutidine	15	13/1	86	99
9[e)]	**C5**	lutidine	65	20/1	83	99
10[f)]	**C5**	lutidine	40	>20/1	79	99
11[g)]	**C5**	lutidine	40	>20/1	77	99
12[h)]	**C5**	lutidine	40	>20/1	86	99
13[h), i)]	**C5**	lutidine	40	>20/1	86	99

[a)] Reactions were conducted with 0.1 mmol of **1a**, 0.2 mmol of **2a**, 0.15 mmol of base, and 20 mol% of catalyst in 0.5 ml of solvent at rt. [b)] Determined by ^{1}H-NMR of the crude reaction mixture. [c)] Isolated yield of **3a**. [d)] Determined by HPLC analysis (using chiral stationary phases). [e)] Benzene was used. [f] EtOAc was used. [g] *i*PrOH was used.

[h] 0.125 mmol of aldehyde **2a** was used. [i] 10 mol% of the catalyst was used. TMS - trimethylsilyl, TBDMS - *tert*-butyldimethylsilyl, MDPS - methyldiphenylsilyl, TPS - triphenylsilyl, lutidine - 2,6-lutidine.

After optimizing the reaction conditions, we began exploring the scope of the organocatalytic cascade reaction by varying BODIPY derivative **1** (Scheme 2, A). We assessed the effect of the electronic properties of the substituents at BODIPY on reactivity and the stereochemical outcome. In general, the reaction tolerates various alkyl substituents at positions 2, 3, and 5, 6 of BODIPY moiety (numbering is showed in Scheme 2), affording the corresponding cyclopropanes **3a-c** in high isolated yields (68-91%) with excellent stereoselectivities (in all cases dr >20/1, and 99% *ee*). Interestingly, the reaction with 2,6-dibromo BODIPY **1d** proceeded with decreased diastereocontrol, which showed that electron-withdrawing substituents could have a deleterious effect. Luckily, substrate **3d** can be prepared in high yield by bromination of **3a** (for more details, please, see late-stage transformations). Additionally, we tested organocatalytic cascade reaction with BODIPY derivatives bearing alkyl substituents at positions 1, and 7. Remarkably, neither the reaction of *trans*-cinnamaldehyde (**2a**) with **1f** gave the corresponding product nor the reaction with unsymmetrically substituted derivative **1e**. Subsequently, the scope of the developed organocascade reaction was investigated by varying enal substrates **2** (Scheme 2, B). In general, high-to-excellent yields of cyclopropanes **3** with excellent enantioselectivities and diastereoselectivities were obtained with aromatic enals bearing electron-donating groups (**3f**, **3i**) and electron-withdrawing groups (**3j-p**) in a *para* position on the aromatic ring. Similarly, *meta*- and *ortho*-substituted aromatic enals afforded the corresponding products in excellent yields with excellent stereochemical outcomes. For example, the reactions of enals, which bear electron-donating groups in various positions of the phenyl ring, give products **3f-i** in excellent isolated yields (above 90%) as single optically pure diastereomers (in all cases dr >20/1, and 99% *ee*). Excellent efficiency of the developed method was also shown in reactions of enals bearing electron-withdrawing groups, especially in reactions of halogenated enals producing BODIPYs **3l-p** with excellent isolated yields (above 89%) and excellent stereochemical outcomes (in all cases dr >20/1, and 99% *ee*). Besides aromatic, heteroaromatic, and aliphatic enals were also explored. We observed slightly decreased diastereocontrol in reactions of heteroaromatic enals. Unfortunately, aliphatic α,β-unsaturated aldehydes bearing γ-protons provided a complex mixture of products.

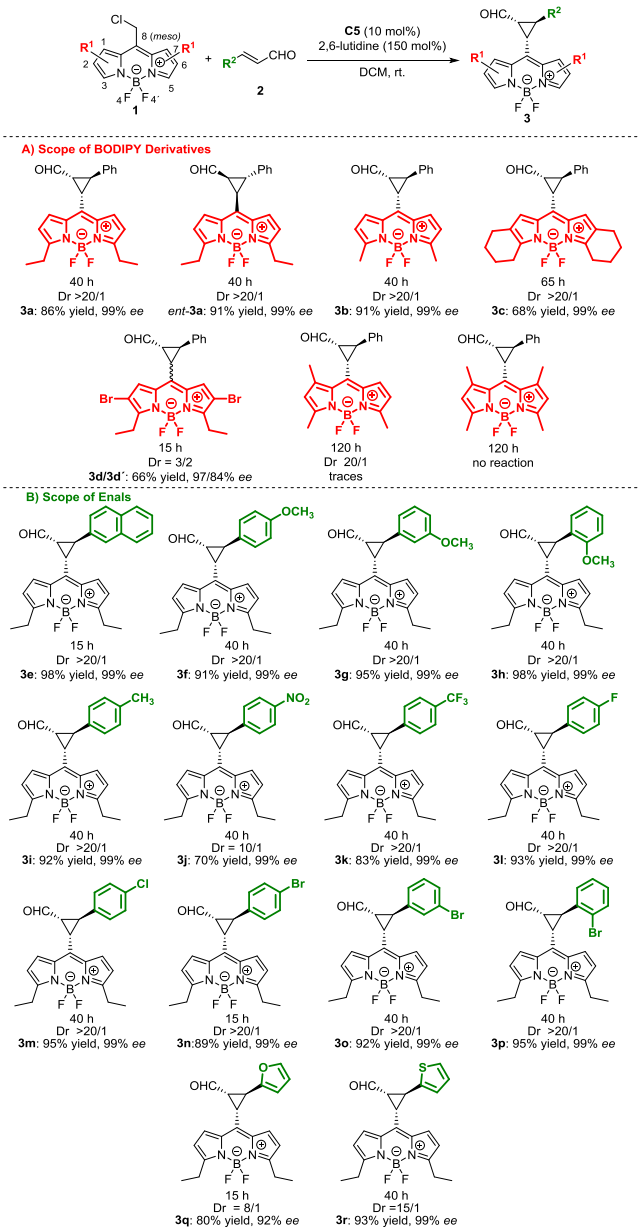

Scheme 2. Substrate scope.

The absolute configuration of **3a** was determined using X-ray diffraction analysis, and the configuration of **3a** was assigned as 1*R*, 2*S*, 3*S* (Figure 2, for details, see the SI file).[20] The absolute configurations of the other BODIPY derivatives **3** were assigned by analogy.

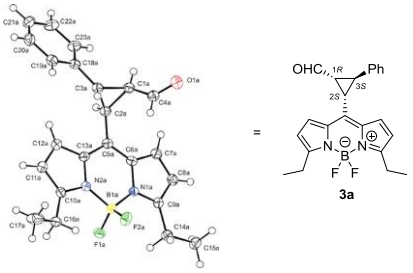

Figure 2. View on one of two symmetrically independent molecules of **3a** with atom numbering scheme, the displacement ellipsoids are drawn on 50% probability level.

Based on the determined absolute configuration and the previous reports, [18b, 19b, 21] a mechanism of the developed organocascade reaction was proposed (Scheme 3). Initially, enal **2a** is activated *via* condensation with the chiral secondary amine generating iminimum intermediate **I**. Subsequently, the formed iminium ion **I** with a shielded *Re*-face is stereoselectively attacked by nucleophilic BODIPY derivative **1** affording enamine **II**. Next, an intramolecular *3-exo-tet* cyclization of enamine **II** results in the formation of cyclopropane intermediate **III**, which upon hydrolysis in the final stage furnishes product **3a** releases a chiral amine back to the catalytic cycle.

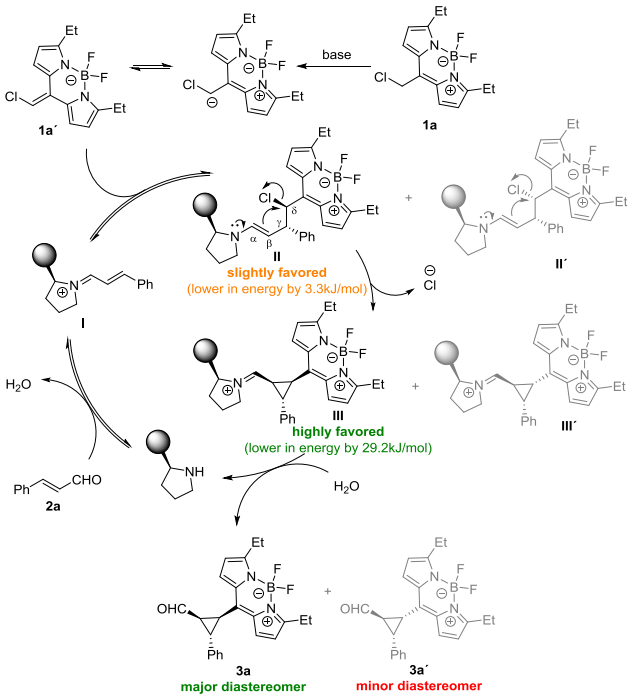

Scheme 3. Proposed reaction mechanism.

The proposed reaction mechanism was verified by DFT computations, which were used to devise the geometry and total energy for intermediates **II** and **III** at the cyclopropanation step. The formation of **II** from **I** and **1a´** decreases the extent of bond delocalization in the chain attached to the pyrrole nitrogen (for more details see the SI). The C–C bonds neighbouring the electronegative chloride become destabilized most, which in turn increases their reactivity. The subsequent reaction step involving chloride cleavage from **II** is favoured further by molecular geometry (directing the nucleophilic chloride towards the open space) and by the favourable distribution of the electrostatic potential (Figure S8). The bonds within the chain attached to the pyrrole nitrogen undergo rearrangements upon chloride cleavage, whereupon geometric changes start to take place. According to Natural Bonding Orbital analysis, the carbon atom losing the chloride group (denoted as C_δ) compensates for the charge loss by becoming the acceptor for the C_β–C_γ bond. Even though the delocalization energy of this interaction is 64.0 kJ/mol and the respective C_β–C_δ Mayer Bond Order (MBO) becomes 0.309 in the initial geometry, this partial bond is already capable to drive the succeeding geometric rearrangements towards the generation of the cyclopropane ring. During the course of this rearrangement, the total energy of the cation decreases by 284 kJ/mol and its C_β–C_δ bond distance becomes shortened from 2.491 Å to 1.544 Å, forming a regular cyclopropane motif within the newly generated **III**. It is noteworthy, that this ring closure is accomplished despite the suboptimal geometry of important carbon atoms (specifically C_β and C_δ) just after chloride abstraction from **III**, meaning that the ring closure will occur for both diastereomers differing in their chloride placement. The necessary geometry rearrangements of the carbon and hydrogen atoms during the cyclization step occur gradually and they achieve proper geometry after arriving to **III**. The generation of cationic **II** is a paramount prerequisite for the cyclization step to be accomplished, since molecular **II** exhibits no tendency for ring closure. The need for cation formation was evidenced by the C_β–C_δ bond MBO, whose computed value -0.038 in molecular **II** suggested no bonding interaction present. It's remarkable, that the cyclization itself is achieved without forming any transition-state molecule of the cation — geometry optimization of cationic **II** led smoothly to **III**, while no proper transition-state molecule from the starting molecular **II** could be obtained. The other diastereomer of **II**, denoted as **II´**, differs in the position of its chloride group on C_δ and is higher by only 3.3 kJ/mol in total energy over **II**. Both these diastereomers are thus capable of existence and will undergo spontaneously cyclopropanation after chloride cleavage. This is in contrast with the possible diastereomer **III´**, where the particular orientation of the BODIPY moiety on the cyclopropane ring exhibits strong preference for a single diastereomer. The reason for this preference lies in the cyclopropane geometry, since its BODIPY moiety is oriented away from the phenyl substituent on the cyclopropane ring in **III**, whereas the proximity of these groups induces significant steric strain in **III'**. Therefore, the latter complex becomes higher by 29.2 kJ/mol in total energy, and its formation is disfavoured.

To demonstrate the synthetic utility of the developed organocascade reaction, we performed a reaction between **1a** and **2a** in gram scale, giving the product **3a** in 89% yield, retained stereochemical outcomes (99% *ee*, and dr >20/1, Scheme 4, A). As an example of subsequent transformations, cyclopropane **3a** was converted to various compounds **3d-8** (Scheme 4, B). Cyclopropane **3a** was selectively brominated at BODIPY core using NBS as an electrophilic source of bromine. Reaction provided the corresponding cyclopropane **3d** in high yield with retained enantioselectivity. That type of post-transformation is indicated as more appropriate compared to organocascade reaction of **1d**. Then, late-stage transformations of aldehydic group of **3a** were performed. For example, **3a** was selectively oxidized

to carboxylic acid **4** using Pinnick oxidation in high yield. Slightly higher yield of the corresponding methyl ester **5** was reached by subsequent methylation using trimethylsilyl-diazomethane. Selective reduction of aldehyde was performed using Luche reduction, which produce alcohol **6** with excellent yield and retained enantiomeric excess (reduction using $NaBH_4$ produced significantly lower yield). Other selected examples of the transformation of cyclopropane **3a** included reductive amination and Wittig olefination. Corresponding *α,β*-unsaturated ester **7** and amine **8a** were prepared in high yields without losing enantiomeric purities.

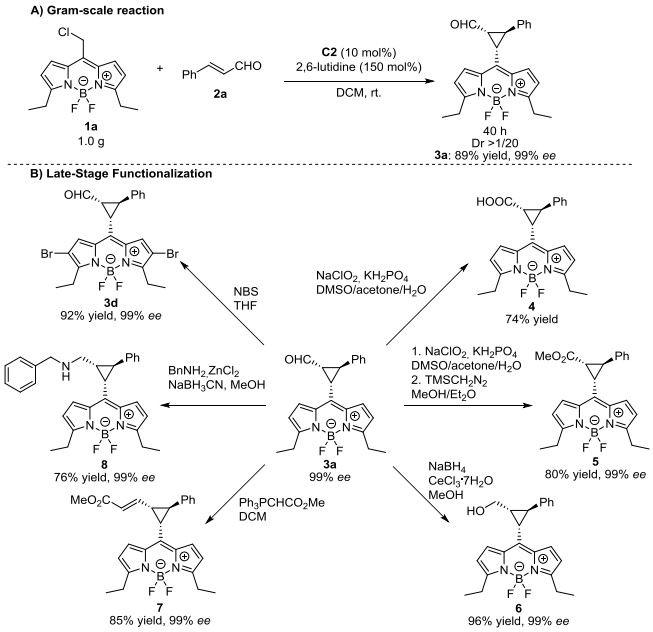

Scheme 4. Gram-scale experiment and late-stage functionalization.

The basic photophysical characterization was performed for all the obtained compounds **3-8**. The main objective of this characterization was to demonstrate the photoactivity and stability of prepared compounds. Absorption and fluorescent spectra for initial substrate **3a** was measured in eight different solvents at $1 \cdot 10^{-5}$ M concentration (Table S6 and Figure S5), and acetonitrile was found as the most convenient for further studies with compounds **3-8**. In all cases, absorption spectra exhibit characteristic BODIPY pattern that can be decomposed into one sharp band due to 0-0 $S_0 \rightarrow S_1$ electronic transition and a shoulder at slightly higher energy due to 0-1 vibrational band of the same transition. Absorption spectra also contains a weaker broad band located between 300 and 400 nm which correspond to the population of higher excited states. Prepared solutions exhibit good stability with no observed precipitation over a two-week period. The main absorption band (compounds **3-8** in CH_3CN) was centred between 511.5 to 552.5 nm and exhibits typical high value of absorption coefficient (see Table 2, and Figure 3). Noteworthy, the absorption maximum is red shifted for the derivatives with modified BODIPY core (**3c**, **3d**), whereas the late-stage functionalization induced a small blue shift (**4**-**8c**). Small blue shift was also observed for **3a** in solvents with high polarity, such as methanol, which corresponds with previously reported observation. [22]

The half width ($fwhm_{abs}$) of the intense absorption band also increases with the substitution at the BODIPY core as well by the substitution of the phenyl group on cyclopropane. The fluorescence spectrum was recorded using the excitation at the corresponding absorption maxima and represents mirror images of the intense absorption bands with small Stokes shift 296-576 cm^{-1}. For both cases of electron-withdrawing

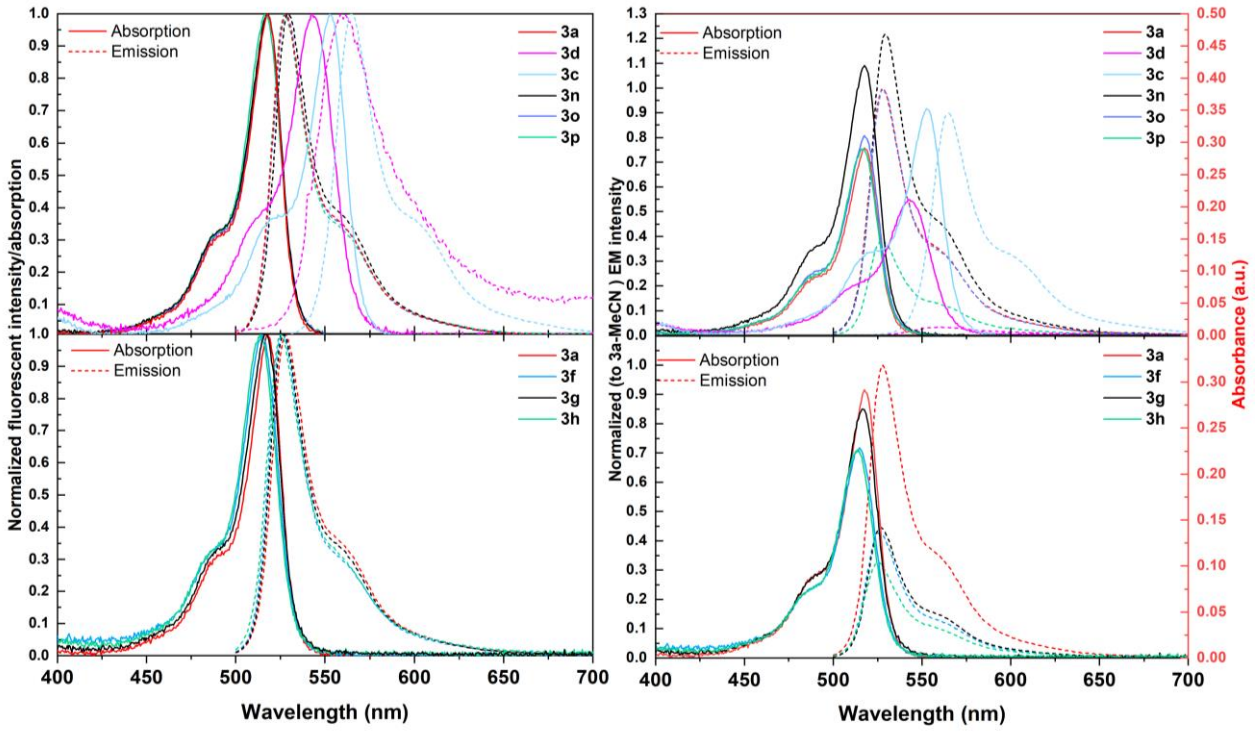

Figure 3. Selected absorption and emission spectra.

(**3n-p**) and electron-donating groups (**3f-h**) was also observed a gap decrease between the absorption and emission maxima. Moreover, the relative intensity of the emission radiation depends on the position of the respective group and decreases in the following order: *para>meta>ortho.* In general, observed emission spectra can be divided into three main groups with respect to the relative emission intensity (emission intensity normalized to the emission of initial **3a** compound). The compounds with significantly lower (E_x/E_{3a} <0.8), almost equal (0.8< E_x/E_{3a} <1.2) and higher (1.2< E_x/E_{3a}) emission intensity (Table 2).

Table 2. Spectral and photophysical properties of BODIPY derivatives, where λ_{abs} is the maximum in absorption spectrum, α is absorption coefficient, *fwhm* is half width of corresponding band, λ_{em} is the maximum in emission spectrum, E_x/E_{3a} is the ratio between the corresponding emission maximum (E_x) and emission maximum of compound **3a** in CH_3CN (E_{3a}) and the Stokes shift is the difference between absorption and excitation maximum.

ID	λ_{abs} (nm)	α (cm^{-1})	*fwhm* (cm^{-1})	λ_{em} (nm)	E_x/E_{3a}	*fwhm* (cm^{-1})	Stok. (cm^{-1})
3a	517.5	0.725	828	528	1	867	384
***ent*-3a**	516.5	0.85	909	530	0.96	827	493
3b	514.5	0.65	934	526	0.90	892	425
3c	552.5	0.875	844	565	0.91	882	400
3d[a]	542.5	0.525	1078	560	0.04	1438	576
3f[a]	514.5	0.575	914	526	0.43	858	425
3g[a]	516.5	0.675	909	527	0.45	889	386
3h[a]	514.5	0.575	916	525	0.32	930	389
3l	517	0.675	886	529	1.14	934	439
3m[b]	518	1.225	886	530	1.23	946	437
3n[b]	517.5	1.05	906	529	1.22	897	420
3o	517.5	0.775	866	528	1.02	867	384
3p[a]	517	0.725	869	527	0.38	870	367
3e	518.5	0.675	789	528	1.11	889	329
3i	516	0.975	891	528	0.97	852	441
3j[a]	518.5	0.45	884	529	0.44	815	383
3k	517.5	0.725	828	528	0.85	886	384
3q[a]	515.5	0.425	989	527	0.31	1061	423
3r[a]	516	0.350	985	529	0.06	1410	441
4[b]	514.5	0.825	780	523	1.34	899	316
5[b]	516.5	1.075	718	527	1.32	852	386
6[b]	511.5	0.6	769	523	1.52	884	430
7[a]	516	0.625	759	524	0.58	933	296

Reported values of observed photoluminescence maxima are significantly lower[a]/higher[b] than **3a** compound as a reference.

The observed changes in the emission properties could be used to monitor the controlled synthesis of individual derivatives or to study the selective reactivity at particular *ortho/meta/para* positions. Together with the expected small value of photoluminescent lifetime (in order of several ns), [22] the prepared compounds may also be applied in the field of bioimaging. [23]

In summary, we have developed a novel organocatalytic approach to enantiopure BODIPY derivatives using organocascade reaction of readily available BODIPY derivatives with *α,β*-unsaturated aldehydes. The reaction is efficiently catalyzed by a chiral secondary amine, affording BODIPY derived cyclopropane carbaldehydes in high yields and excellent stereoselectivity. This outcome was thoroughly studied using DFT calculations of intermediates, which are responsible for the stereochemistry of final products. The synthetic utility was demonstrated on selected post-functionalization reactions of enantiopure products. The basic set of photophysical properties was studied at all prepared chiral BODIPY derivatives, showing promising properties for the application, which are ongoing in our laboratories.

Experimental Section

The catalyst **C5** (6.0 mg, 0.01 mmol, 0.1 eq.) was added to a solution of the corresponding *α,β*-unsaturated aldehyde **2** (0.125 mmol, 1.25 eq.) in DCM (0.5 ml). The mixture was stirred for 10 minutes at room temperature. Then, 2,6-lutidine (17.4 µl, 0.15 mmol, 1.5 eq.) and BODIPY **1** (0.1 mmol, 1.0 eq.) were added. The reaction was stirred for the indicated time (TLC control). With complete conversion of **1**, the solvents were evaporated. The crude product was purified by column chromatography (eluting by hexane/EtOAc mixtures).

Acknowledgements

V.D. gratefully acknowledges Charles University Grant Agency (1350120) for financial support. J.V. gratefully acknowledges the Czech Science Foundation (20-29336S) for financial support. J.H. acknowledges support of the European Regional Development Fund and the state budget of the Czech Republic, project BIATRI, No. CZ.02.1.01/0.0/0.0/15_003/0000445 and the grant SVV-2020-260590. The authors also thank Dr. Štícha and Dr. Urban for the MS and IR analysis.

References

[1] a) N. Boens, B. Verbelen, M. J. Ortiz, L. Jiao, W. Dehaen, *Coord. Chem. Rev*. **2019**, *399*, 213024; b) J. Bañuelos *Chem. Rec.* **2016**, *16*, 335-348; c) G. Ulrich, R. Ziessel, A. Harriman, *Angew. Chem., Int. Ed.* **2008**, *47*, 1184-1201; d) A. Loudet, K. Burgess, *Chem. Rev.* **2007**, *107*, 4891-4932.

[2] a) A. P. Demchenko in *Introduction to Fluorescence Sensing*; Springer International Publishing, Switzerland, **2020**; b) S. V. Mulay, T. Yudhistira, M. Choi, Y. Kim, J. Kim, Y. J. Jang, S. Jon, D. G. Churchill, *Chem. - An Asian J.* **2016**, *11*, 3598-3605; c) N. Boens, V. Leen, W. Dehaen, *Chem. Soc. Rev.* **2012**, *41*, 1130-1172.

[3] J. Chan, S. C. Dodani, C. J. Chang, *Nat. Chem.* **2012**, *4*, 973-984.

[4] L. Zhao, H. Zhou, Q. Zhou, C. Peng, T. Cheng, G. Liu, *Sensors Actuators B Chem.* **2020**, *320*, 128383.

[5] H. Lu, J. Mack, T. Nyokong, N. Kobayashi, Z. Shen, *Coord. Chem. Rev.* **2016**, *318*, 1-15.

[6] F. Zinna, L. Di Bari, *Chirality* **2015**, *27*, 1-13.

[7] Q. Yang, M. Fusè, J. Bloino, *Front. Chem.* **2020**, *8*, 801.

[8] C. Wolf, K. W. Bentley, *Chem. Soc. Rev.* **2013**, *42*, 5408-5424.

[9] R. G. Clarke, M. J. Hall, *Adv. Heterocycl. Chem.* **2019**, *128*, 181-261.

[10] a) C. Maeda, S. Nomoto, K. Takaishi, T. Ema, *Chem. – A Eur. J.* **2020**, *26*, 13016-13021; b) Z. Liu, Z. Jiang, C. He, Y. Chen, Z. Guo, *Dye. Pigment.* **2020**, *181*, 108593; c) F. Pop, N. Zigon, N. Avarvari, *Chem. Rev.* **2019**, *119*, 8435-8478. d) X. Gao, X. Qin, X. Yang, Y. Li, P. Duan, *Chem. Commun*. **2019**, *55*, 5914-5917; e) C. Maeda, K. Nagahata, K. Takaishi, T. Ema, *Chem. Commun.* **2019**, *55*, 3136-3139; f) J. Jiménez, L. Cerdán, F. Moreno, B. L. Maroto, I. García-Moreno, J. L. Lunkley, G. Muller, S. de la Moya, *J. Phys. Chem. C*, **2017**, *121*, 5287-5292; g) M. Toyoda, Y. Imai, T. Mori, *J. Phys. Chem. Lett.* **2017**, *8*, 42-48; h) S. Abbate, T. Bruhn, G. Pescitelli, G. Longhi, *J. Phys. Chem. A* **2016**, *121*, 394-400; i) S. Feuillastre, M. Pauton, L. Gao, A. Desmarchelier, A. J. Riives, D. Prim, D. Tondelier, B. Geffroy, G. Muller, G. Clavier, G. Pieters, *J. Am. Chem. Soc.* **2016**, *138*, 3990-3993; j) Y. Wu, S. Wang, Z. Li, Z. Shen, H. Lu, *J. Mater. Chem. C* **2016**, *4*, 4668-4674; k) L. Zhang, L. Zhao, K. Wang, J. Jiang, *Dye. Pigment.*, **2016**, *134*, 427-433; l) E. M. Sánchez-Carnerero, F. Moreno, B. L. Maroto, A. R. Agarrabeitia, M. J. Ortiz, B. G. Vo, G. Muller, S. de la Moya, *J. Am. Chem. Soc.* **2014**, *136*, 3346-3349; m) E. M. Sánchez-Carnerero, F. Moreno, B. L. Maroto, A. R. Agarrabeitia, J. Bañuelos, T. Arbeloa, I. López-Arbeloa, M. J. Ortiz, S. de la Moya, *Chem. Commun.* **2013**, *49*, 11641-11643; n) I. Móczár, P. Huszthy, Z. Maidics, M. Kádár, K. Tóth, *Tetrahedron* **2009**, *65*, 8250-8258; o) A. Gossauer, F. Nydegger, T. Kiss, R. Sleziak, H. Stoeckli-Evans, *J. Am. Chem. Soc.* **2004**, *126*, 1772-1780.

[11] a) T. Ono, K. Ishihama, A. Taema, T. Harada, K. Furusho, M. Hasegawa, Y. Nojima, M. Abe, Y. Hisaeda, *Angew. Chem., Int. Ed.* **2021**, *60*, 2614-2618; b) P. Moneva Lorente, A. Wallabregue, F. Zinna, C. Besnard, L. Di Bari, J. Lacour, *Org. Biomol. Chem.* **2020**, *18*, 7677-7684; c) V. G. Jiménez, F. M. Santos, S. Castro-Fernández, J. M. Cuerva, P. M. P. Gois, U. Pischel, A. G. Campana, *J. Org. Chem.* **2018**, *83*, 14057-14062; d) R. Clarke, K. L. Ho, A. A. Alsimaree, O. J. Woodford, P. G. Waddell, J. Bogaerts, W. Herrebout, J. G. Knight, R. Pal, T. J. Penfold, M. J. Hall, *ChemPhotoChem* **2017**, *1*, 513-517; e) Y. Gobo, M. Yamamura, T. Nakamura, T. Nabeshima, *Org. Lett.* **2016**, *18*, 2719-2721; f) T. Bruhn, G. Pescitelli, F. Witterauf, J. Ahrens, M. Funk, B. Wolfram, H. Schneider, U. Radius, M. Bröring, *Eur. J. Org. Chem.* **2016**, 4236-4243; g) R. I. Lerrick, T. P. L. Winstanley, K. Haggerty, C. Wills, W. Clegg, R. W. Harrington, P. Bultinck, W. Herrebout, A. C. Benniston, M. J. Hall, *Chem. Commun.* **2014**, *50*, 4714-4716; h) A. Gossauer, F. Fehr, F. Nydegger, H. Stöckli-Evans, *J. Am. Chem. Soc.* **1997**, *119*, 1599-1608.

[12] M. Meazza, C. M. Cruz, A. M. Ortuño, J. M. Cuerva, L. Crovetto, R. Rios, *Chem. Sci.* **2021**, *12*, 4503-4508; b) T. Rigotti, J. Asenjo-Pascual, A. Martín-Somer, P. Milán Rois, M. Cordani, S. Díaz-Tendero, Á. Somoza, A Fraile, J. Alemán, *Adv. Synth. Catal.* **2020**, *362*, 1345-1355; c) A. Guerrero-Corella, J. Asenjo-Pascual, T. J. Pawar, S. Díaz-Tendero, A. Martín-Sómer, C. V. Gómez, J. L. Belmonte-Vázquez, D. E. Ramírez-Ornelas, E. Peña-Cabrera, A. Fraile, D. C. Cruz, J. Alemán, *Chem. Sci.* **2019**, *10*, 4346-4351.

[13] T. T. Talele, *J. Med. Chem.* **2016**, *59*, 8712-8756.

[14] Y. Y. Fan, X. H. Gao, J. M. Yue, *Sci. China Chem.* **2016**, *59*, 1126-1141.

[15] a) G. A. Molander, J. P. Burke, P. J. Carroll, *J. Org. Chem.* **2004**, *69*, 8062-8069; b) Y. Okada, T. Minami, T. Yamamoto, J. Ichikawa, *Chem. Lett.* **1992**, *21*, 547-550.

[16] a) Z. Hang, J. Zhu, X. Lian, P. Xu, H. Yu, S. Han, *Chem. Commun*. **2016**, *52*, 80-83; b) N. Yu, S. Han, H. Yu, *Tetrahedron* **2015**, *71*, 4665-4669; c) Y. Zhang, J. Zhu, N. Yu, H. Yu, *Chinese J. Chem.* **2015**, *33*, 171-174; d) H. Yu, M. Liu, S. Han, *Tetrahedron* **2014**, *70*, 8380-8384; e) S. Hanessian, Z. Shao, J. S. Warrier, *Org. Lett.* **2006**, *8*, 4787-4790; f) P. H. Y. Cheong, K. N. Houk, J. S. Warrier, S. Hanessian, *Adv. Synth. Catal.* **2004**, *346*, 1111-1115; g) S. Hanessian, U. Reinhold, G. Gentile, *Angew. Chem., Int. Ed.* **1997**, *36*, 1881-1884.

[17] C. Apel, M. Christmann, *Tetrahedron* **2021**, *80*, 131760; and references therein.

[18] *Selected seminal works on cyclopropanations:* a) I. Ibrahem, G. L. Zhao, R. Rios, J. Vesely, H. Sundén, P. Dziedzic, A. Córdova, *Chem. - A Eur. J.* **2008**, *14*, 7867-7879; b) R. Rios, H. Sundén, J. Vesely, G. L. Zhao, P. Dziedzic, A. Córdova, *Adv. Synth. Catal.* **2007**, *349*, 1028-1032. c) H. Xie, L. Zu, H. Li, J. Wang, W. Wang, *J. Am. Chem. Soc.* **2007**, *129*, 10886-10894; d) S. H. McCooey, T. McCabe, S. J. Connon, *J. Org. Chem.* **2006**, *71*, 7494-7497; e) R. K. Kunz, D. W. C. MacMillan, *J. Am. Chem. Soc.* **2005**, *127*, 3240-3241; f) C. D.

Papageorgiou, M. A. Cubillo De Dios, S. V. Ley, M. J. Gaunt, *Angew. Chem., Int. Ed.* **2004**, *43*, 4641-4644; g) N. Vignola, B. List, *J. Am. Chem. Soc.* **2004**, *126*, 450-451; h) S. Arai, K. Nakayama, T. Ishida, T. Shioiri, *Tetrahedron Lett.* **1999**, *40*, 4215-4218.

[19] a) V. Dočekal, A. Vopálenská, P. Měrka, K. Konečná, O. Jand´ourek, M. Pour, I. Císařová, J. Veselý, *J. Org. Chem.* **2021**, *86*, 12623-12643; b) V. Dočekal, S. Petrželová, I. Císařová, J. Veselý, *Adv. Synth. Catal.* **2020**, *362*, 2597-2603; c) M. Meazza, M. E. Light, A. Mazzanti, R. Rios, *Chem. Sci.* **2016**, *7*, 984-988; d) M. Meazza, M. Ashe, H. Y. Shin, H. S. Yang, A. Mazzanti, J. W. Yang, R. Rios, *J. Org. Chem.* **2016**, *81*, 3488-3500.

[20] CCDC 2047587 (**3a**) contains the supplementary crystallographic data for this paper. These data can be obtained free of charge from The Cambridge Crystallographic Data Centre via www.ccdc.cam.ac.uk/data_request/cif

[21] J. Vesely, G. L. Zhao, A. Bartoszewicz, A. Córdova, *Tetrahedron Lett.* **2008**, *49*, 4209-4212.

[22] K. Zlatić, H. B. E. Ayouchia, H. Anane, B. Mihaljević, N. Basarić, T. Rohand, *J. Photochem. Photobiol. A Chem.* **2020**, *388*, 112206.

[23] P. Kaur, K. Singh, *J. Mat. Chem. C.* **2019**, *7*, 11361-11405.

Stereoselective Cyclopropanation of BODIPY Derivatives by an Organocascade Reaction

Adv. Synth. Catal. **Year**, *Volume*, Page – Page

Vojtěch Dočekal, Tereza Koberová, Jan Hrabovský, Róbert Gyepes, Ivana Císařová, Ramon Rios, Jan Veselý*